

LABORATORY STUDY



Endoplasmic reticulum stress participates in the pathophysiology of mercury-caused acute kidney injury

Plácido Rojas-Franco^a , Margarita Franco-Colín^a , Alejandra Paola Torres-Manzo^b , Vanessa Blas-Valdivia^c , María del Rocio Thompson-Bonilla^d , Sinan Kandir^e  and Edgar Cano-Europa^a 

^aLaboratorio de Metabolismo I Departamento de Fisiología, Escuela Nacional de Ciencias Biológicas, Instituto Politécnico Nacional, Ciudad de México, México; ^bDepartment of Molecular Physiology and Biophysics, Vanderbilt University, Nashville, TN, USA; ^cLaboratorio de Neurobiología, Departamento de Fisiología, Escuela Nacional de Ciencias Biológicas, Instituto Politécnico Nacional, Ciudad de México, México; ^dLaboratorio de Medicina Genómica. Hospital Regional 1ro. de Octubre. ISSSTE, Ciudad de México, México; ^eDepartment of Physiology, Ceyhan Faculty of Veterinary Medicine, Cukurova University, Adana, Turkey

ABSTRACT

Acute exposure to mercury chloride (HgCl₂) causes acute kidney injury (AKI). Some metals interfere with protein folding, leading to endoplasmic reticulum stress (ERS), and the activation of cell death mechanisms, but in the case of mercury, there is no knowledge about whether the ERS mediates tubular damage. This study aimed to determine if HgCl₂ causes an AKI course with temporary activation of ERS and if this mechanism is involved in kidney cell death. Male mice were intoxicated with 5 mg/kg HgCl₂ and sacrificed after 24, 48, 72, and 96 h of mercury administration. The kidneys of euthanized mice were used to assess the renal function, oxidative stress, redox environment, antioxidant enzymatic system, cell death, and reticulum stress markers (PERK, ATF-6, and IRE1 α pathways). The results indicate temporary-dependent renal dysfunction, oxidative stress, and an increase of glutathione-dependent enzymes involved in the bioaccumulation process of mercury, as well as the enhancement of caspase 3 activity along with IRE1 α , GADD-153, and caspase 12 expressions. Mercury activates the PERK/eIF2 α branch during the first 48 h. Meanwhile, the activation of PERK/ATF-4 branch allowed for ATF-4, ATF-6, and IRE1 α pathways to enhance GADD-153. It led to the activation of caspases 12 and 3, which mediated the deaths of the tubular and glomerular cells. This study revealed temporary-dependent ERS present during AKI caused by HgCl₂, as well as how it plays a pivotal role in kidney cell damage.

ARTICLE HISTORY

Received 30 May 2019
Revised 18 October 2019
Accepted 20 October 2019

KEYWORDS

Mercury nephrotoxicity;
acute kidney injury;
mercury chloride;
endoplasmic reticulum
stress; unfolded
protein response




1. Introduction

Mercury (Hg) is a heavy metal used in the agriculture, mining, pharmaceutical, and chemistry industries. It exists in many chemical forms as organic salts (methyl- or ethyl-mercury), inorganic salts (HgCl₂), or a vapor [1,2]. Over time, several intoxications with all chemical forms of this metal have been documented. However, inorganic mercury salts produce greater renal damage than other mercury chemical forms do. Particularly, HgCl₂ causes acute kidney injury (AKI), and it is the most common model for studying renal toxicity mechanisms [3–5].

Several biochemical mechanisms are involved in cell injury caused by mercury. One of the most crucial mercury toxicity mechanisms is its binding to the sulfhydryl group present in proteins. Also, HgCl₂ reduced glutathione (GSH), cysteine (Cys), and homocysteine (Hcy)

concentration into the cells. In the kidney, some transport mechanisms bioaccumulate mercury complexes with thiols, such as organic anion transporters 1 and 3 (OAT1/OAT3) and system b⁰⁺. It causes oxidative stress, cytoskeletal structure alterations, and cell damage [6,7]. Also, HgCl₂ enhances the Sirt1/Nrf2/OH-1 pathway, which does not compensate for oxidative stress. Moreover, mercury chloride reduces ATP synthesis and the activities of Na⁺-K⁺-ATPase, Mg²⁺-ATPase, Ca²⁺-ATPase, and Ca²⁺-Mg²⁺-ATPase. If the sodium and calcium gradients change, the kidney cells suffer cell death characterized by tubular necrosis, glomerular sclerosis, and interstitial inflammatory cell infiltration [5,8].

Also, some reports link mercury poisoning with organelle dysfunction, such as mitochondria, cytoskeleton, and endoplasmic reticulum, both *in vivo* and

CONTACT Edgar Cano-Europa  ecano@ipn.mx,  edgarcanoeuropa@yahoo.com.mx  Laboratorio de Metabolismo I, Departamento de Fisiología, Escuela Nacional de Ciencias Biológicas, Instituto Politécnico Nacional. Av. Wilfrido Massieu s/n, Esq. Manuel L. Estampa, Colonia Unidad Profesional Adolfo López Mateos, Alcaldía Gustavo A. Madero, Ciudad de México, CP. 07738, México

© 2019 The Author(s). Published by Informa UK Limited, trading as Taylor & Francis Group.

This is an Open Access article distributed under the terms of the Creative Commons Attribution License (<http://creativecommons.org/licenses/by/4.0/>), which permits unrestricted use, distribution, and reproduction in any medium, provided the original work is properly cited.

in vitro [7–10]. However, concerning the endoplasmic reticulum, a pathway that correlates this organelle with AKI caused by mercury has not been described. Still, some reports show that mercury and other heavy metals can interfere with proper protein folding in the endoplasmic reticulum, which can be a significant detriment to cell survival [11]. Unfolded or misfolded protein accumulation is associated with several cellular stressors, such as redox environment disturbance, a Ca^{2+} imbalance, altered protein glycosylation, or protein folding defects; it is known as endoplasmic reticulum stress (ERS) [12]. Meanwhile, the unfolded protein response (UPR) is a process that seeks to restore the endoplasmic reticulum's normal function through multiple strategies mediated by the initial activation of ER membrane-associated sensors, PKR-like ER-kinase (PERK), activating transcription factor 6 (ATF6), and the inositol-requiring enzyme-1 α (IRE1 α). When the UPR is not enough to restore the organelle homeostasis, the cells activate cell-death mechanisms that are primarily mediated by the action of the UPR protein growth arrest, the deoxyribonucleic acid damage-inducible gene 153 (GADD-153, also known as CHOP), and ER membrane-associated caspase 12 [12,13].

Nowadays, there are no reports about the relationship between AKI and ERS caused by mercury chloride. However, we propose that there is a direct association between mercury and ERS in the kidney because in an *in vitro* model using an NRK-52E kidney cell culture, HgCl_2 increases the GRP78 expression (an ERS sensor) [14]. Also, in the brain, there are studies to correlate the three pathways of ERS (IRE1 α , ATF-4, PERK) and organic mercury toxicity [15].

Thus, the aim of this study was the establishment of a temporal relationship between AKI caused by HgCl_2 and the processes of oxidative stress, ERS, and cell death.

2. Materials and methods

2.1. Animals housing conditions and experimental design

We used 60 albino male mice between 25 and 30 g. They housed in a cooled room ($21 \pm 2^\circ\text{C}$) with 12/12-h light cycles, relative humidity of 40–60%, and food and water *ad libitum*. All experimental procedures described in this study follow the Mexican Official Standard NOM-082-ZOO-1999 as well as the Guide for the Care and Use of Laboratory Animals from the National Research Council (US) Committee (National Research Council (US) Committee for the Update of the Guide for the Care and Use of Laboratory Animals, 2011). Also, the protocol

received approval from the Internal Bioethics Committee (CEI-ENCB) with number approbation CEI-ENCB 019/2014.

The animals were divided into two groups: the control group ($n = 12$) received a 0.9% saline solution (SS) intraperitoneally (ip), and the treated group ($n = 48$) received a single dose of HgCl_2 (5 mg/kg; ip). Twelve animals from each group were euthanized with pentobarbital monosodic (90 mg/kg ip) at 24, 48, 72, and 96 h after mercury intoxication. Meanwhile, the control group was euthanized at 96 h using the same drug. Before euthanizing, six animals underwent renal function evaluation using a metabolic cage for 6 h without food and water as previously described [16]. The urine and serum samples were used to evaluate renal function. The next six animals from each group were euthanized without renal function evaluation, and we dissected the kidneys. The left kidneys were frozen and kept at -70°C until use, whereas the right kidneys were fixed in 4% paraformaldehyde in PBS.

2.2. Renal function evaluation

We employed a commercially available assay kit (*Spinreact* company, Girona, Spain) to evaluate the glucose, creatinine, and protein in the urine, as well as the BUN, uric acid, and creatinine in serum.

2.3. Biochemical and molecular determinations

We used frozen kidneys homogenized in 3 mL of 10 mM of phosphate buffer pH 7.4, and then, they were used to assess all of the oxidative stress markers, the enzymatic activities, the caspase 3 activity, and the western blot assays. The protein concentration was determined by using the Bradford method [17].

2.4. Quantification of oxidative stress markers

We assessed the lipid peroxidation (LP), reactive oxygen species (ROS), oxidized glutathione (GSSG), and nitrite (NO_2) quantifications as oxidative stress markers as previously described with some modification [18,19].

2.5. Evaluation of the antioxidant enzymatic system (SOD, catalase, and total SOD) and some enzymes associated with the toxicity of mercury (glutathione-S-transferase, γ -glutamyl transpeptidase and myeloperoxidase)

Spectrophotometrical techniques were used to evaluate all enzyme activities as previously described [18,20,21] with some modification to the microplate evaluation

with the Multiskan GO (Thermo Scientific, Waltham, MA).

For glutathione reductase (GR) activity, 2 μ L of the homogenate was added to 100 μ L to 100 mM of phosphate buffer (pH 7.0) containing 1 mM of GSSG and 0.1 mM of NADPH. The reaction was monitored at a temperature of 37 °C for 10 min. The results are expressed as mmoles of NADPH used/mg protein/min.

For the catalase activity, we used 5 μ L of cell extract to 3 mL of 100 mM phosphate buffer, pH 7.4, containing 30 mM of H₂O₂. The absorbance was recorded at 240 nm after 10 min at 37 °C. The decomposition of H₂O₂ by the catalase present in the samples followed first-order kinetics according to the equation of $k = 2.3 t \log A_0/A$, where k is the first-order reaction rate constant, t is the time over which the decrease of hydrogen peroxide caused by catalase activity was measured (10 min), and A_0/A is the ratio of optical densities at times 0 and 10 min. Catalase activity is expressed as k/mg of protein.

The SOD activity was measured spectrophotometrically; 5 μ L of cell extract was mixed with 2.9 mL of a solution containing 10 μ M NaN₃, 10 μ M of reduced cytochrome c, and 1 mM of EDTA dissolved in 20 mM of sodium bicarbonate and 0.02% Triton X-100, pH 10.2. The enzymatic assay was started by the addition of 50 μ L of xanthine oxidase (3.4 mg/mL in 0.1 mM of EDTA). The change in absorbance was monitored every 30 s at 550 nm for 3 min. One unit of SOD activity is the amount of enzyme that decreased the reduction rate of cytochrome c by 50%. The SOD activity is expressed as U/mg of protein for glutathione-S-transferase (GST). 5 μ L of the homogenate was added to 100 μ L of 0.1 M of Tris-HCl, pH 8.2, containing 10 mM of GSH. The mixture was incubated for 1 min at 37 °C. After that, 5 μ L of 50 mM of 1-chloro-2,4-dinitrobenzene was added, and we monitored the absorbance at 340 nm for 3 min. One unit (U) of GST caused the formation of 1 μ mol of S-2,4-dinitrophenyl glutathione, using its molar extinction coefficient ($\epsilon_{340} = 10 \text{ mM}^{-1} \text{ cm}^{-1}$). Thus, GST activity is expressed as U/mg protein/min.

For γ -glutamyl transpeptidase (γ -GT), we used 5 μ L of the cell homogenate, which was added to 100 μ L of 100 mM of Tris-HCl, pH 8.0, containing 1 mM of γ -glutamyl *p*-nitroaniline and 20 mM of glycylglycine. The mixture was incubated at 37 °C, and we monitored the absorbance at 410 nm for 4 min. The molar extinction coefficient of *p*-nitroaniline formed was used to express the results as mmol *p*-nitroaniline formed/mg protein/min ($\epsilon_{410} = 8800 \text{ M}^{-1} \text{ cm}^{-1}$).

For myeloperoxidase (MPO) activity, 2 μ L of the homogenate was added to 160 μ L of 90 mM of a citrate

buffer (pH 4.5) containing 0.1% Triton X-100 and 0.65 mM of O-dianisidine. The reaction started with the addition of 40 μ L of 0.43 mM of H₂O₂. The mixture was incubated at 37 °C. We monitored the absorbance at 460 nm for 15 min, and at 460 nm for 5 min. The molar extinction coefficient of *p*-nitroaniline formed was used to express the results as mmoles O-dianisidine oxidized/mg protein/min ($\epsilon_{460} = 11.3 \text{ mM}^{-1} \text{ cm}^{-1}$).

2.6. Endoplasmic reticulum stress evaluation

We evaluated the ERS by quantifying the expression of some intermediaries from the PERK, ATF-6, and IRE1 pathways through western blot assays as previously described [18]. Briefly, 50 μ g of protein was charged in 10% polyacrylamide gels and separated by electrophoresis, then electrotransferred to PVDF membranes in a semidry chamber. After that, proteins of gels were electrotransferred to PVDF membranes in a semidry chamber. Transferred membranes were blocked for 1 h under constant stirring in PBST (PBS with 0.05% tween 20 with 5% low-fat milk). Blocked membranes were incubated at 4 °C overnight in a blocking buffer containing the primary antibodies of ATF-6 α , GADD34, XBP-1, GADD 153, eIF2 α (Santa Cruz Biotechnology, Santa Cruz, CA: sc-22799, sc-8327, sc-575 and sc-7160, sc-30882, respectively), and caspase-12 (Millipore, AB3613, Burlington, MA) diluted 1:500, as well as IRE1 α Abcam, ab37073) and ATF-4 (Biorbyt, orb-129518) diluted 1:1000 and 1:2000, respectively. After incubation, blots were washed three times with fresh PBST (20 min. per wash) and then incubated in a 1:2000 diluted secondary antibody (HPR-conjugated goat anti-rabbit or rabbit anti-goat; Life technologies, Rockford, IL; 65-6120, 611620, respectively) for 1 h at room temperature under constant stirring. Then, membranes were washed three times with PBST, and finally, protein bands were revealed in photographic plates (JUAMA, México) by chemiluminescence, using Luminata TM Forte from Millipore). Protein β -actin expression was used as a charge control and constitutive protein (Santa Cruz Biotechnology; sc-1615, dilution: 1:4000). The optical density (O. D.) from all bands obtained was analyzed by Image J program (NIH, Bethesda, MD; version 1.51p), according to program specifications. Proteins O. D. are expressed as a protein/ β -actin ratio.

2.7. Caspase 3 activity assay

Caspase 3 activity was assessed by using a commercial caspase 3 colorimetric assay kit (Millipore, APT165) as previously described [16].

2.8. Histological analysis

The kidney fixed with paraformaldehyde was embedded in paraffin, and 5- μ m slices were obtained with a standard microtome. One section was stained with hematoxylin–eosin (HE), dehydrated, and mounted in resin. Meanwhile, another section was incubated with annexin V-Cy3 (100 μ g/ml, Millipore) for 15 min in darkness. The photomicrographs were acquired with Nikon-50i, and they were digitalized and analyzed with an NIS element program.

2.9. Statistical analysis

All data are presented as mean \pm standard error of the mean, and they were analyzed by one-way analysis of variance (one-way ANOVA) and the Student–Newman–Keuls *post hoc* test. Values with $p < 0.05$ were considered to be statistically different.

3. Results

Table 1 shows the effect of HgCl₂ on renal function markers during the progress of HgCl₂ intoxication. It shows an increase of BUN, serum uric acid, serum creatinine, glycosuria, and proteinuria with a reduction in the clearance creatinine since 24 h after mercury intoxication.

Table 2 shows the quantification of ROS, lipid peroxidation (LP) and nitrites (NO₂), and glutathione oxidized (GSSG) in the kidney. The GSSG was the first metabolite

that increased by about 37–56% from 24 h to 96 h after HgCl₂ intoxication. The ROS and NO₂ levels enhanced from 48 h after mercury administration about threefold and twofold, respectively. Meanwhile, HgCl₂ caused an increase of the LP at 72 and 96 h, about 150 and 212%, respectively.

Table 3 shows the results of antioxidant enzyme activity. Catalase presented a time-dependent decay in its activity, whereas GR and MPO progressively raised their activities between 60 and 500%, respectively. We found a twofold increase in γ GT activity starting at 24 h after intoxication. Meanwhile, GST presented a two-fold increased activity only at 48 h but remained unchanged for the rest of the time. The total SOD was not affected by HgCl₂ intoxication during the 96 h after intoxication.

Figure 1 shows that the PERK branch had a high activity from 24 h to 72 h after mercury intoxication because we found a higher expression of eIF2 α (Figure 1(A)) from 48 h (44% more expression than control) to 96 h (64% more expression than control) with a maximum expression at 72 h (110% compared with the control expression) after mercury intoxication. Also, the GADD-34 expression (Figure 1(B)) had higher expression with respect to the control from 24 h about 21%, with maximum expression at 72 h after mercury chloride intoxication about 89% with respect to the control group. Concerning ATF-4 (Figure 1(C)), its expression increased since 48 h after HgCl₂ administration (30% more expression than the control group) until 96 h (79% more expression than control).

Table 1. Temporal evaluation of functional renal markers in the acute kidney injury induced with HgCl₂.

Group	Serum BUN (mg/dL)	Serum uric acid (mg/dL)	Urine glucose (mg/dL)	Urine proteins (mg/dL)	Serum creatinine (mg/dL)	Urine creatinine (mg/dL)	Creatinine clearance (mL/min)
HgCl ₂							
Control	31.94 \pm 4.28 ^a	2.08 \pm 0.14 ^a	55.03 \pm 6.48 ^a	7.46 \pm 0.70 ^a	1.24 \pm 0.19 ^a	28.35 \pm 8.22	0.75 \pm 0.23 ^a
24 h	73.10 \pm 10.9 ^b	4.53 \pm 0.08 ^b	113.7 \pm 4.43 ^b	22.28 \pm 4.63 ^b	2.58 \pm 0.45 ^b	48.89 \pm 7.13	0.17 \pm 0.068 ^b
48 h	81.14 \pm 4.13 ^{b,c}	5.44 \pm 0.61 ^{b,c}	423 \pm 74.94 ^c	21.94 \pm 2.82 ^b	2.41 \pm 0.31 ^b	60.56 \pm 8.40	0.24 \pm 0.036 ^b
72 h	123 \pm 11.32 ^d	5.65 \pm 0.21 ^{b,d}	308.5 \pm 100.8 ^{c,d}	19.46 \pm 2.11 ^b	2.06 \pm 0.12 ^b	30 \pm 10.75	0.26 \pm 0.029 ^b
96 h	190 \pm 27.14 ^e	5.46 \pm 0.19 ^{b,e}	451.2 \pm 8.63 ^{c,e}	17.57 \pm 0.87 ^b	3.56 \pm 0.71 ^c	30.67 \pm 14.66	0.13 \pm 0.034 ^b
<i>p</i>	<0.001	<0.001	0.012	0.003	0.012	0.128	0.004
<i>F</i> _{4,25}	17.733	22.759	4.039	5.217	4.039	1.983	5.125

Data represent the mean \pm SEM. a \neq b \neq c \neq d \neq e. One-way ANOVA, Student–Newman–Keuls *post hoc* ($n = 6$).

Table 2. Temporal evaluation of the oxidative stress markers in the acute kidney injury induced with HgCl₂.

Group	Lipid peroxidation (URF/ mg protein)	ROS quantification (ng of DCF/mg protein/h)	GSSG content (μ g of GSSG/ mg protein)	NO ₂ quantification μ g of NO ₂ /mg protein
Control	1.023 \pm 0.003 ^a	338.50 \pm 32.18 ^a	1.63 \pm 0.09 ^a	0.312 \pm 0.01 ^a
HgCl ₂				
24 h	1.146 \pm 0.090 ^a	435.51 \pm 126.60 ^a	2.24 \pm 0.13 ^b	0.404 \pm 0.07 ^a
48 h	1.220 \pm 0.040 ^a	658.52 \pm 5.78 ^b	2.55 \pm 0.20 ^b	0.514 \pm 0.03 ^b
72 h	2.565 \pm 0.230 ^b	617.80 \pm 2.41 ^b	2.52 \pm 0.14 ^b	0.519 \pm 0.02 ^b
96 h	3.200 \pm 0.100 ^c	854.10 \pm 18.59 ^c	2.33 \pm 0.13 ^b	0.575 \pm 0.06 ^b
<i>p</i>	<0.001	<0.001	<0.001	0.002
<i>F</i> _{4,25}	67.284	11.702	6.819	5.625

Data represent the mean \pm SEM. a \neq b \neq c. One-way ANOVA, Student–Newman–Keuls *post hoc* ($n = 6$).

Table 3. Temporal evaluation of the antioxidant enzymatic system and the enzymes involved in the acute kidney injury induced with HgCl₂.

Group	Glutathione reductase activity (mmol of NADPH consumed/mg protein/min)	Catalase activity (k/mg protein)	Total SOD (U SOD/mg protein)	GST activity (U GST/mg protein)	γ-GT activity (mmol of NBA formed/mg protein/min)	MPO activity (mmol of o-dianisidine oxidized/mg protein/min)
HgCl ₂						
Control	35.53 ± 2.21 ^a	1.74 ± 0.04 ^a	41.82 ± 4.99 ^a	1.75 ± 0.09 ^a	0.525 ± 0.06 ^a	0.05 ± 0.001 ^a
24 h	42.76 ± 1.84 ^b	0.93 ± 0.02 ^b	38.52 ± 9.36 ^a	1.80 ± 0.28 ^a	1.064 ± 0.10 ^b	0.13 ± 0.005 ^b
48 h	46.10 ± 2.1 ^b	0.92 ± 0.01 ^b	44.13 ± 6.01 ^a	2.93 ± 0.36 ^b	0.786 ± 0.01 ^b	0.14 ± 0.003 ^b
72 h	45.40 ± 2.95 ^b	0.99 ± 0.03 ^b	44.25 ± 1.90 ^a	2.48 ± 0.18 ^a	0.712 ± 0.02 ^b	0.10 ± 0.003 ^c
96 h	56.71 ± 2.30 ^c	0.69 ± 0.01 ^c	41.09 ± 10.50 ^a	1.72 ± 0.37 ^a	0.926 ± 0.14 ^b	0.30 ± 0.012 ^d
<i>p</i>	<0.001	<0.001	0.979	0.014	<0.001	<0.001
<i>F</i> _{4,25}	10.908	258.27	0.107	3.839	6.274	234.840

Data represent the mean ± SEM. *a* ≠ *b* ≠ *c*. One-way ANOVA, Student–Newman–Keuls *post hoc* (*n* = 6).

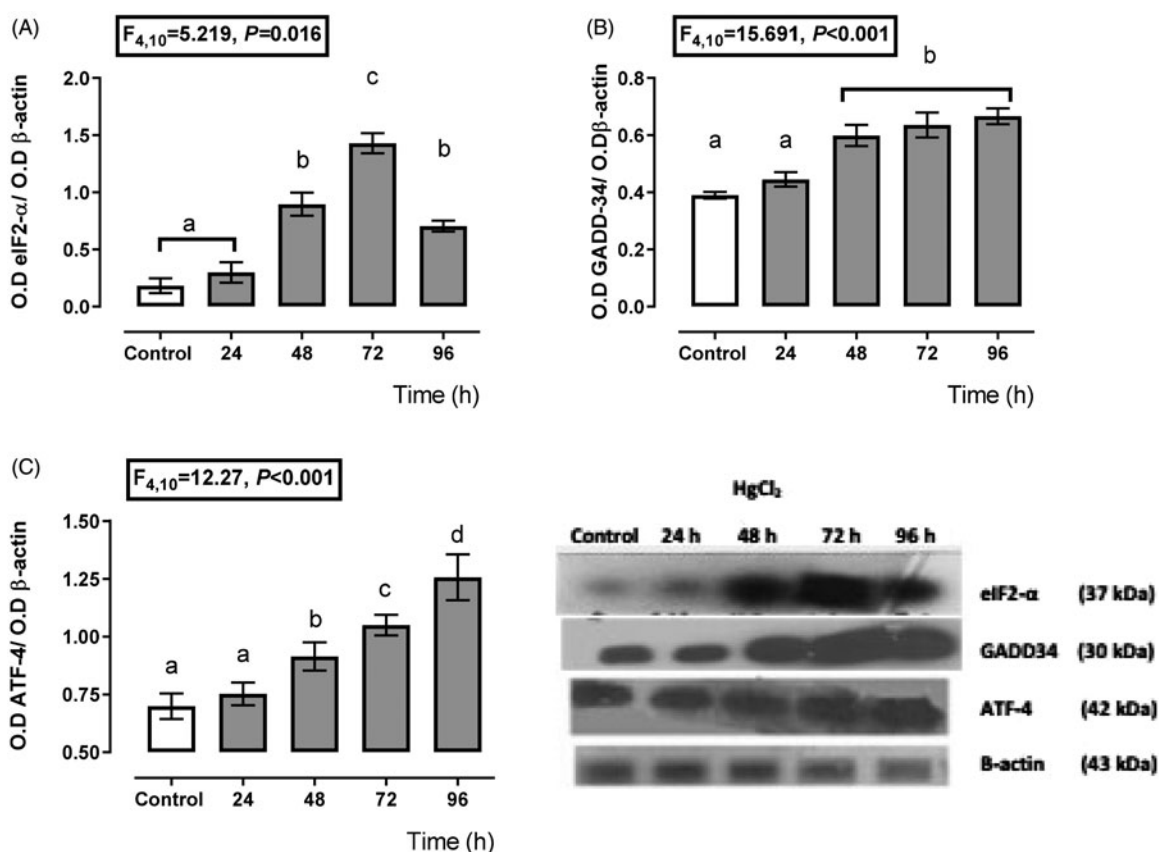


Figure 1. Time-dependent expression of endoplasmic reticulum stress markers, eIF2- α (A), GADD-34 (B), and ATF-4 (C) in the HgCl₂-associated acute kidney injury. Data represents the mean ± SEM. One-way repeated measures ANOVA. Student–Newman–Keuls *post hoc* test. *n* = 6 *a* ≠ *b* ≠ *c* ≠ *d* ≠ *e*.

Figure 2 shows a transient depending over-expression of the IRE-1 α and ATF6 branches. The expression of IRE-1 α (Figure 2(A)), XBP-1 (Figure 2(B)), and ATF6 (Figure 2(C)) increased about 112–198%, 32–155%, and 22–161%, respectively, from 24 to 96 h after HgCl₂ administration. However, the higher expression for XBP-1 and ATF6 was after 96 h of mercury intoxication (about 155 and 161% overexpression with respect to the control group); meanwhile, the higher IRE-1 α

expression was at 72 h (198%), and it decayed at 96 h (118%) after mercury intoxication.

Figure 3 shows the expression of cell-death promoter protein GADD-153 (Figure 3(A)) and endoplasmic reticulum-associated caspase 12 (Figure 3(B)) and the effector caspase 3 activity (Figure 2(C)). It showed a higher expression for GADD-153 and caspase 12 as well as effector caspase 3 activity from 24 to 72 h, and they decayed at 96 h after mercury intoxication.

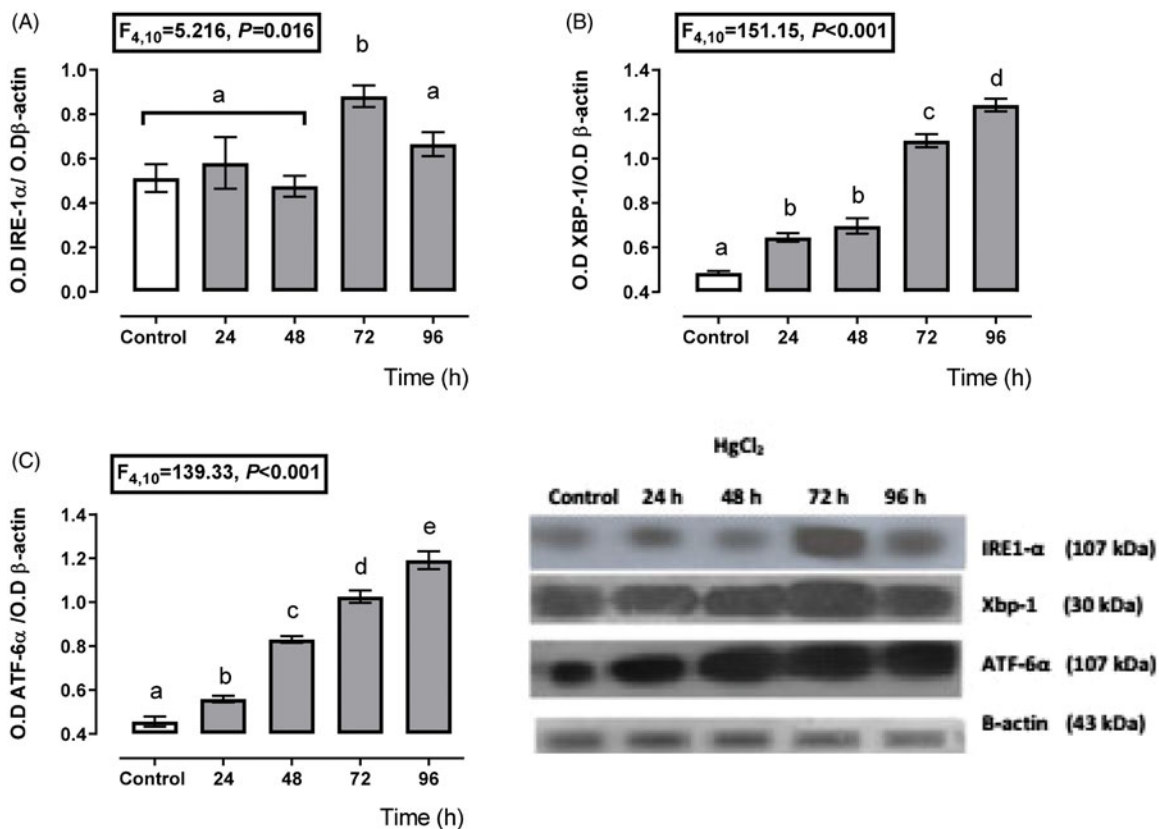


Figure 2. Time-dependent expression of endoplasmic reticulum stress markers IRE-1 α (A), XBP-1 (B), and ATF-6 α (C) in the HgCl₂-associated acute kidney injury. Data represents the mean \pm SEM. One-way ANOVA. Student–Newman–Keuls *post hoc* test. $n = 6$ $a \neq b \neq c \neq d \neq e$.

Also, **Figure 4** shows the histological analysis of the kidney of the mice intoxicated with inorganic mercury. It showed transient cellular damage since 24 h after mercury intoxication. The damage observed in the hematoxylin–eosin stain was edema, cellular atrophy of distal and proximal tubules, distortion of cellular continuity, nucleus loss, and hyperchromatic nuclei. Even so, the immunofluorescence against annexin-V marked by a red fluorescent marker presented a transient overexpression for 24 h.

4. Discussion

Some reports demonstrate the relationship between mercury toxicity and ERS. It is well known that mercury can bind to native proteins and inhibit their biological activity by oxidizing and covalently bound with sulfhydryl groups from functional side chains, or also by displacing enzymes cofactors. All of these events promote renal dysfunction; our results show that HgCl₂ causes AKI because it reduces in a temporary course the clearance creatine with an increase of uric acid, BUN, glycosuria, and proteinuria.

One of the responses of the kidney cells against mercury chloride intoxication is the overexpression of heat-shock proteins (HSP) and glucose-regulated proteins (GRP), with the purpose of enhancing the degradation of misfolded and unfolded proteins. Additionally, it increases the expression of genes encoding many other ER proteins to prevent the excessive accumulation of unfolded or misfolded proteins. The result above reveals that mercury enhanced the expression of these proteins as GADD34, and it is in accordance with other research groups that found that in the rat, the administration of HgCl₂ enhances the expression of HSP72, HSP60, and GRP75, which are critical players in the assembling, transport, and refolding of proteins during oxidative damage [14,22–24]. However, there were no studies relating these events with the activation of the three pathways of ERS. Our results suggest that HgCl₂KI partially activated the PERK pathway during the first 48 h through the activation of two pathways.

One pathway involved PERK-immediate substrate nuclear factor erythroid 2-related factor 2 (Nrf2). Nrf2 is independent of eIF2 α phosphorylation, and it is one of the primary regulators of cytoprotective responses to

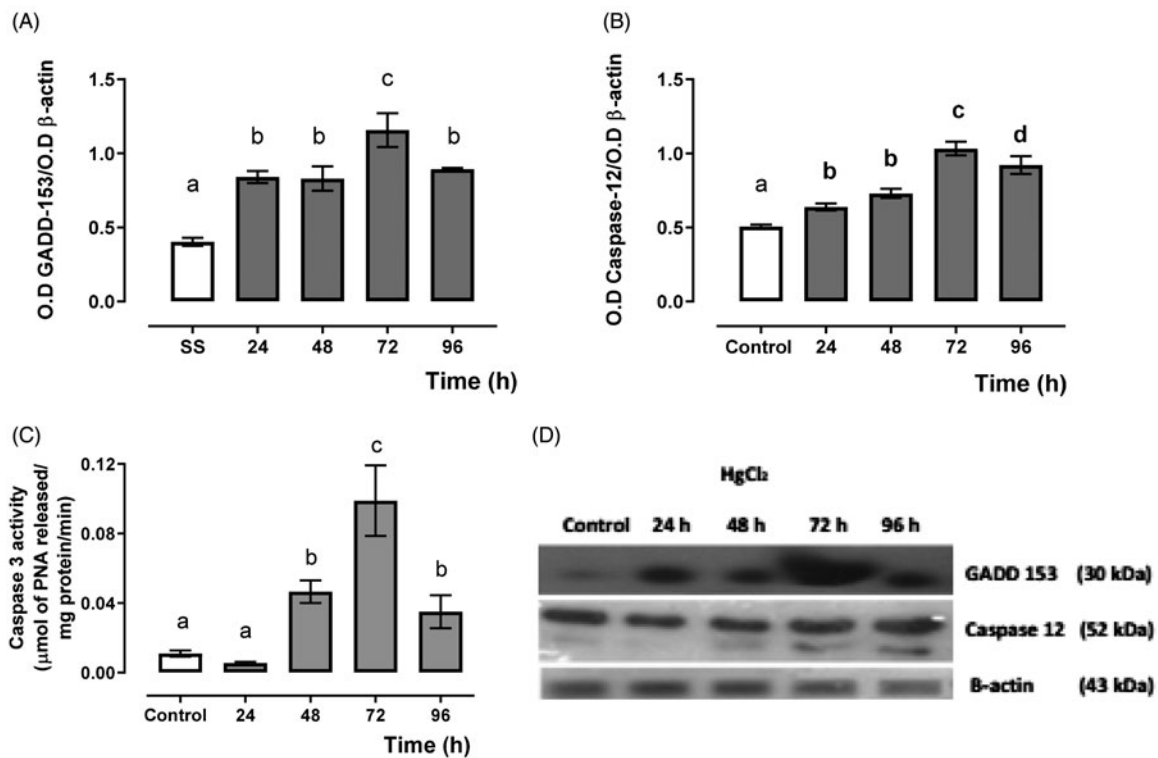


Figure 3. Time-dependent GADD-153 (A), caspase 12 expression (B) and caspase 3 activity (C), and representative blots of the Western blot technique, and (D) in the HgCl₂-associated acute kidney injury. Data represents the mean ± SEM. One-way ANOVA. Student–Newman–Keuls *post hoc* test. *n* = 6 *a* ≠ *b* ≠ *c* ≠ *d*.

oxidative stress, as we can observe in the result above [25–27]. Thus, Nrf2 could act as a potent activator for the transcription of antioxidant enzymes like glutathione S-transferase (GST) and GR as we can observe in the temporary result of this study, particularly 48 h after mercury intoxication [28,29]. These mechanisms have a relationship with mercury bioaccumulation process in kidney cells more than antioxidants or detoxifying compensatory action. Moreover, it has an association between GADD153 and oxidative stress process because it induces the overexpression and over-activity of endoplasmic reticulum oxidoreductin 1 (ERO-1) which enhances H₂O₂ production and cytoplasm Ca²⁺ overload to promotes oxidative stress [30,31]. Also, it has been reported that Sirt1/Nrf2/OH-1 pathway is insufficient to respond to the mercury chloride causes oxidative stress because HgCl₂ blocks positive feedback loop Sirt1/Keap1/Nrf2/ARE that is an antioxidant pathway [8].

The second mechanism involved the phosphorylating eIF2 α which attenuates global protein translation and also it activates ATF-4-dependent transcription. We proposed that the second route is progressively activating from 48 h until 72 h because there is a rise in the expression of ATF-4, which can induce the expression

of GADD-34, a protein that is associated with protein phosphatase 1 (PP1) and promotes dephosphorylation of eIF2 α [32]. Thus, it attenuates the PERK/eIF2 α pathway to promote cell death. After 72 h of mercury intoxication, ATF-4 and GADD-153 have the same pattern of expression. Thus ATF-4 mediated GADD-153 translation through GADD 34 [33]. Meanwhile, GADD34 is a target molecule of ATF6 and IRE1 α pathways. In our result, IRE1 α had the same pattern expression of GADD34, but ATF6 presented a stepwise expression increase, and so did XBP-1. These molecular mechanisms promote the synthesis of new ERS mediators and cell-death promoters like GADD-153 [34,35]. 72 h after mercury exposition, the apoptosis process is activated because the IRE1 α kinase domain forms a complex with adaptor protein TNF receptor-associated factor 2 (TRAF2), the apoptosis signal regulator kinase 1 (ASK1), and the c-Jun kinases (JNK) [36]. This hypothesis is supported because mercury reduces the expression of BCL₂ and BCL_{XL} with an increase of BAX, BAK, and caspase-12 [8,16,37]. This molecular event participates in the formation of the mitochondrial transition pore (MTP), which allows the release of cytochrome c from mitochondria to the cytoplasm to form the apoptosome [10]. This idea is supported because our results show

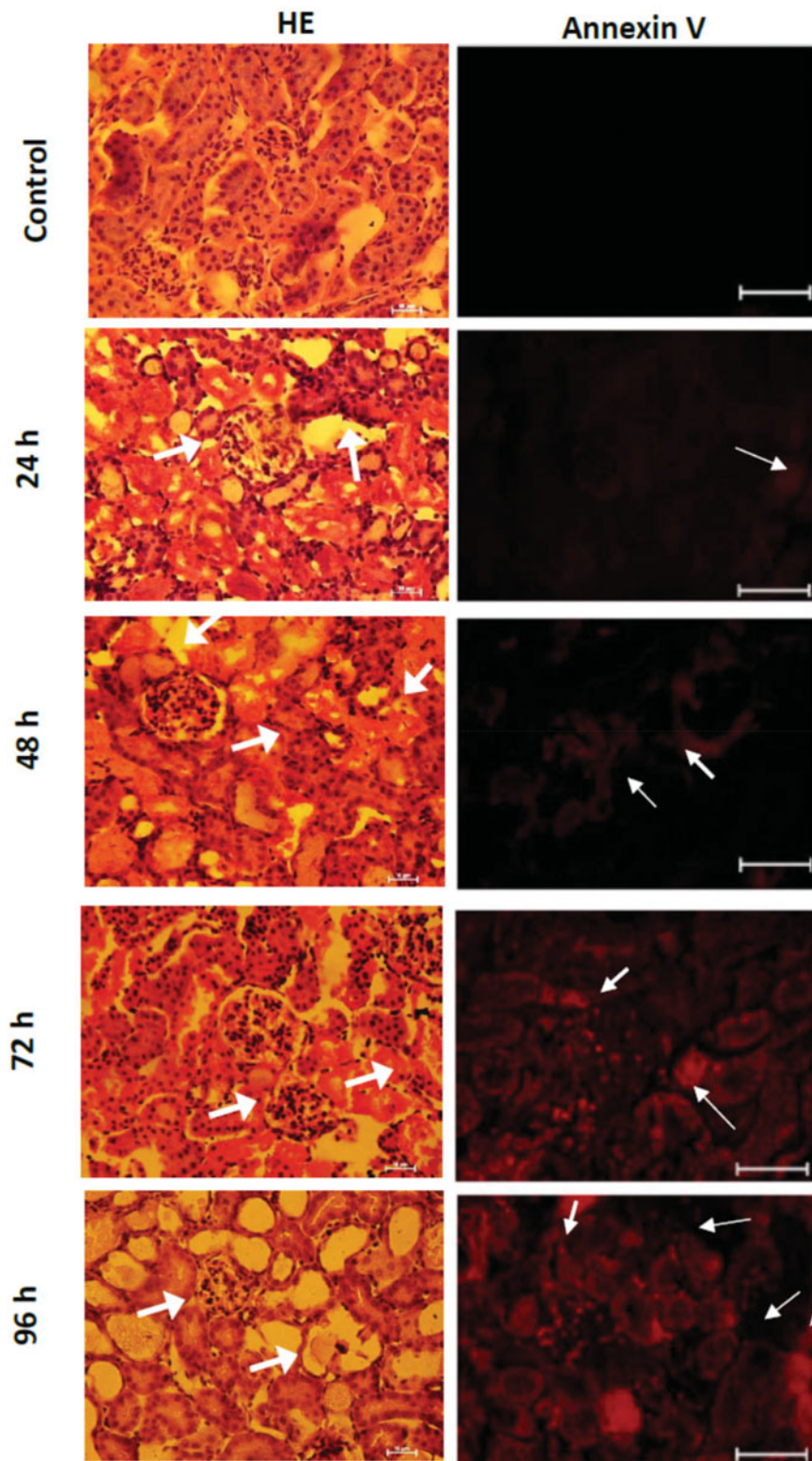


Figure 4. Temporal evaluation of the morphological changes in the HgCl_2 -associated acute kidney injury. The arrows show in HE stain photomicrographs the cellular atrophy of distal and proximal tubules, distortion of cellular continuity, nucleus loss, and hyperchromatic nuclei. Meanwhile, the annexin V positive cells are observed in red.

the overexpression pattern of GAD153 agrees with the expression of caspase 12 and the over-activity of caspase 3.

Finally, the increase of the oxidative and ERS promotes the over-expression of annexin-V with evident histological damage characterized by in the hematoxylin-eosin stain was edema, the cellular atrophy of distal and proximal tubules, distortion of cellular continuity, nucleus loss, and hyperchromatic nuclei. All of these biochemical, molecular, and morphological change promotes renal dysfunction.

5. Conclusion

We conclude that ERS participates in HgCl_2 caused AKI because the PERK/eIF2 α branch is activated during the first 48 has a protective but not effective response. Also, the activation of the PERK/ATF-4 branch allows that ATF-4, ATF-6, and IRE1 α pathways activate a cell-death promoter response through GADD-153 and the subsequent activation of caspases 12 and 3, which mediate the death and renal dysfunction.

Acknowledgments

Edgar Cano-Europa thanks COTEBAL-IPN for the support given this year for the realization of this project. The authors thank INSTITUTO POLITÉCNICO NACIONAL, SECRETARÍA DE INVESTIGACIÓN Y POSGRADO-IPN, and CONACyT for financial support. The researchers are fellows of EDI, COFAA, and SNI.

Disclosure Statement

The authors declare that there is no conflict of interest for this study.

Funding

This study was partially supported by CONACyT [221057] and SIP-IPN [20195584, 20195320, and 20196304].


ORCID

Plácido Rojas-Franco  <http://orcid.org/0000-0002-3465-9212>

Margarita Franco-Colín  <http://orcid.org/0000-0003-0869-1945>

Alejandra Paola Torres-Manzo  <http://orcid.org/0000-0001-6499-4129>

Vanessa Blas-Valdivia  <http://orcid.org/0000-0002-0977-9829>

María del Rocío Thompson-Bonilla  <http://orcid.org/0000-0002-0977-9829>

Sinan Kandir  <http://orcid.org/0000-0002-8404-7994>

Edgar Cano-Europa  <http://orcid.org/0000-0002-3536-5590>

References

- [1] Li P, Yang Y, Xiong W. Impacts of mercury pollution controls on atmospheric mercury concentration and occupational mercury exposure in a hospital. *Biol Trace Elem Res.* 2015;168:330–334.
- [2] Li Y. Environmental contamination and risk assessment of mercury from a historic mercury mine located in southwestern China. *Environ Geochem Health.* 2013;35:27–36.
- [3] Ye BJ, Kim BG, Jeon MJ, et al. Evaluation of mercury exposure level, clinical diagnosis and treatment for mercury intoxication. *Ann Occup Environ Med.* 2016; 28:5.
- [4] Liu J, Lu YF, Li WK, et al. Mercury sulfides are much less nephrotoxic than mercury chloride and methylmercury in mice. *Toxicol Lett.* 2016;262:153–160.
- [5] Zalups RK. Molecular interactions with mercury in the kidney. *Pharmacol Rev.* 2000;52:113–144.
- [6] Bridges CC, Zalups RK. Transport of inorganic mercury and methylmercury in target tissues and organs. *J Toxicol Environ Health B Crit Rev.* 2010;13:385–410.
- [7] Orr SE, Barnes MC, Joshee L, et al. Potential mechanisms of cellular injury following exposure to a physiologically relevant species of inorganic mercury. *Toxicol Lett.* 2019;304:13–20.
- [8] Li S, Jiang X, Luo Y, et al. Sodium/calcium overload and Sirt1/Nrf2/OH-1 pathway are critical events in mercuric chloride-induced nephrotoxicity. *Chemosphere.* 2019;234:579–588.
- [9] Buelna-Chontal M, Franco M, Hernandez-Esquivel L, et al. CDP-choline circumvents mercury-induced mitochondrial damage and renal dysfunction. *Cell Biol Int.* 2017;41:1356–1366.
- [10] Vergilio CS, Carvalho CEV, Melo E. Mercury-induced dysfunctions in multiple organelles leading to cell death. *Toxicol Vitro.* 2015;29:63–71.
- [11] Tamás MJ, Sharma SK, Ibstedt S, et al. Heavy metals and metalloids as a cause for protein misfolding and aggregation. *Biomolecules.* 2014;4:252–267.
- [12] Gallazzini M, Pallet N. Endoplasmic reticulum stress and kidney dysfunction. *Biol Cell.* 2018;110:205–216.
- [13] Szegezdi E, Logue SE, Gorman AM, et al. Mediators of endoplasmic reticulum stress-induced apoptosis. *EMBO Rep.* 2006;7:880–885.
- [14] Stacchiotti A, Morandini F, Bettoni F, et al. Stress proteins and oxidative damage in a renal derived cell line exposed to inorganic mercury and lead. *Toxicology.* 2009;264:215–224.
- [15] Liu W, Yang T, Xu Z, et al. Methylmercury induces apoptosis through ROS-mediated endoplasmic reticulum stress and mitochondrial apoptosis pathways activation in rat cortical neurons. *Free Radic Res.* 2019;53: 26–44.
- [16] Rojas-Franco P, Franco-Colín M, Camargo MEM, et al. Phycobiliproteins and phycocyanin of *Arthrospira maxima* (*Spirulina*) reduce apoptosis promoters and glomerular dysfunction in mercury-related acute kidney injury. *Toxicol Res Appl.* 2018;2:239784731880507.
- [17] Bradford MM. A rapid and sensitive method for the quantitation of microgram quantities of protein

- utilizing the principle of protein-dye binding. *Anal Biochem.* 1976;72:248–254.
- [18] Torres-Manzo AP, Franco-Colín M, Blas-Valdivia V, et al. Hypothyroidism causes endoplasmic reticulum stress in adult rat hippocampus: a mechanism associated with hippocampal damage. *Oxid Med Cell Longev.* 2018;2018:2089404.
- [19] Blas-Valdivia V, Ortiz-Butrón R, Pineda-Reynoso M, et al. *Chlorella vulgaris* administration prevents HgCl₂-caused oxidative stress and cellular damage in the kidney. *J Appl Phycol.* 2011;23:53–58.
- [20] Ortiz-Butrón R, Blas-Valdivia V, Franco-Colin M, et al. An increase of oxidative stress markers and the alteration of the antioxidant enzymatic system are associated with spleen damage caused by methimazole-induced hypothyroidism. *Drug Chem Toxicol.* 2011;34:180–188.
- [21] Cano-Europa E, López-Galindo GE, Hernández-García A, et al. Lidocaine affects the redox environment and the antioxidant enzymatic system causing oxidative stress in the hippocampus and amygdala of adult rats. *Life Sci.* 2008;83:681–685.
- [22] Goering PL, Fisher BR, Noren BT, et al. Mercury induces regional and cell-specific stress protein expression in rat kidney. *Toxicol Sci.* 2000;53:447–457.
- [23] Stacchiotti A, Lavazza A, Rezzani R, et al. Mercuric chloride-induced alterations in stress protein distribution in rat kidney. *Histol Histopathol.* 2004;19:1209–1218.
- [24] Sharma SK, Goloubinoff P, Christen P. Heavy metal ions are potent inhibitors of protein folding. *Biochem Biophys Res Commun.* 2008;372:341–345.
- [25] Cullinan SB, Zhang D, Hannink M, et al. Nrf2 is a direct PERK substrate and effector of PERK-dependent cell survival. *Mol Cell Biol.* 2003;23:7198–7209.
- [26] Ma Q. Role of Nrf2 in oxidative stress and toxicity. *Annu Rev Pharmacol Toxicol.* 2013;53:401–426.
- [27] Liu W, Xu Z, Li H, et al. Protective effects of curcumin against mercury-induced hepatic injuries in rats, involvement of oxidative stress antagonism, and Nrf2-ARE pathway activation. *Hum Exp Toxicol.* 2017;36:949–966.
- [28] Harvey C, Thimmulappa R, Singh A, et al. Nrf2-regulated glutathione recycling independent of biosynthesis is critical for cell survival during oxidative stress. *Nat Rev Cancer.* 2009;15:443–453.
- [29] Espinosa-Diez C, Miguel V, Mennerich D, et al. Antioxidant responses and cellular adjustments to oxidative stress. *Redox Biol.* 2015;6:183–197.
- [30] Li G, Mongillo M, Chin KT, et al. Role of ERO1- α -mediated stimulation of inositol 1,4,5-triphosphate receptor activity in endoplasmic reticulum stress-induced apoptosis. *J Cell Biol.* 2009;186:783–792.
- [31] Zito E. ERO1: a protein disulfide oxidase and H₂O₂ producer. *Free Radic Biol Med.* 2015;83:299–304.
- [32] Novoa I, Zeng H, Harding HP, et al. Feedback inhibition of the unfolded protein response by GADD34-mediated dephosphorylation of eIF2 α . *J Cell Biol.* 2001;153:1011–1022.
- [33] Tsuru A, Imai Y, Saito M, et al. Novel mechanism of enhancing IRE1 α -XBP1 signalling via the PERK-ATF4 pathway. *Sci Rep.* 2016;6:24217.
- [34] Li M, Baumeister P, Roy B, et al. ATF6 as a transcription activator of the endoplasmic reticulum stress element: thapsigargin stress-induced changes and synergistic interactions with NF-Y and YY1. *Mol Cell Biol.* 2000;20:5096–5106.
- [35] Li Y, Guo Y, Tang J, et al. New insights into the roles of CHOP-induced apoptosis in ER stress structure and properties of C/EBP homologous protein roles of CHOP in ER stress-mediated apoptosis. *Acta Biochim Biophys Sin.* 2014;46:629–640.
- [36] Kim H, Tu HC, Ren D, et al. Stepwise activation of BAX and BAK by tBID, BIM, and PUMA initiates mitochondrial apoptosis. *Mol Cell.* 2009;36:487–499.
- [37] Shenker BJ, Guo TL, Shapiro IM. Mercury-induced apoptosis in human lymphoid cells: evidence that the apoptotic pathway is mercurial species dependent. *Environ Res.* 2000;84:89–99.